Thermochimica Acta, 54 (1982) 59–70
Elsevier Scientific Publishing Company, Amsterdam—Printed in The Netherlands

POLARIZATION EFFECTS IN THE ELECTRICAL CONDUCTIVITY OF OIL SHALES

K. RAJESHWAR

Department of Electrical Engineering, Colorado State University, Fort Collins, CO 80523 (U.S.A.)

(Received 10 September 1981)

ABSTRACT

The d.c. current–voltage characteristics of oil shale samples from the Green River formation and the New Albany deposits, were investivated. The effect of two variable parameters, namely temperature (25–500°C) and shale oil yield (68–340 l tonne^{-1}) on the degree of non-linearity in the current–voltage behavior was examined. An increase in temperature and shale oil yield was found to enhance non-linear current–voltage behavior. This result was interpreted in terms of variations in the bulk conductivity of the shale sample induced by changes in temperature or organic content. A higher intrinsic electrical conductivity results in impediment in the discharge of charge carriers at the electrodes. The consequent space-charge polarization distorts the field distribution within the sample and thereby induces non-linear current–voltage behavior. Another key factor influencing current–voltage behavior is compositional homogeneity of the shale sample. Pyrolyzed shale samples containing carbonaceous residue interspersed with the mineral matrix, comprise a high degree of carbon/mineral particle contacts. These contacts represent an additional source of impedance to carrier motion (under an electric field) and regions of space-charge polarization within the bulk sample. The resultant field distortion is high enough to induce non-linear current–voltage behavior unlike the case of homogeneous materials where such effects usually result in linear polarization.

INTRODUCTION

There has been much recent discussion on the possibility of using electrical techniques for the extraction of the energy-rich organic matter from fossil fuels in general and from oil shales in particular. The majority of the schemes that have been proposed relate to in-situ applications. The possibility of locating burn-fronts by propagating electrical (e.g. radio-frequency) energy through an in-situ process bed offers an attractive alternative to methods based on direct temperature measurement; particularly since temperature sensors such as thermocouples are prone to failure in the hostile environments typical of fossil-fuel process beds [1]. The viability of electrical methods for applications related to extraction and diagnostics in fossil-fuel technology will be contingent upon a thorough understanding of the electrical properties of the source material. To this end, we have previously studied the a.c. electrical properties [2,3] and d.c. electrical conductivity [3,4] of Green River oil shales. In this paper, we present our results on current–voltage relationships in

0040-6031/82/0000–0000/$02.75

oil shales from the eastern and western United States. The variable parameters for these experiments were temperature and shale oil yield. Factors underlying the various polarization mechanisms are discussed in terms of the observed dependence of current density on applied voltage.

POLARIZATION MECHANISMS

It is generally recognized that when an electrical field is applied to a solid material, the current flowing through it is time-dependent. Two types of polarization mechanisms have been invoked to explain this time-dependent effect [5,6].

Linear polarization

In this case, the current density shows a linear relationship with the applied field (i.e. Ohm's law is obeyed). This type of polarization is believed to be caused by dipolar relaxation mechanisms involving the microscopic displacement of bound charges (either in atoms, molecules, or in the crystal lattice of the material) under the influence of the applied electric field. For linear polarization, as pointed out by Sutter and Nowick [5], the "true" conductivity, σ_{true}, of the material is given by the relationship

$$\sigma_{true} = \frac{J_0 - J_{trans}}{E_a} = \frac{J_\infty}{E_a} = \sigma_\infty \tag{1}$$

where the terms J_0 and J_∞ are defined in Fig. 1 and represent the initial and final current density, respectively, J_{trans} is the transient current caused by the dielectric relaxation effect, E_a is the applied field and σ_∞ is the final, steady-state conductivity.

Dielectric relaxation effects, caused by accumulation and resultant separation of mobile charges at the phase (or grain) boundaries in a material are also expected to obey eqn. (1) because the field distortion caused by such polarization mechanisms is often too small to affect E_a appreciably. However, the extent of this distortion may

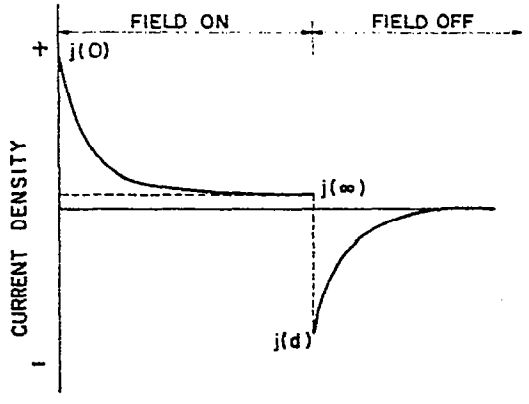

Fig. 1. Variation of current density with time. See text for definition of symbols.

be high enough to induce non-linearity particularly in heterogeneous materials such as oil shales (vide infra).

A further manifestion of linear polarization mechanisms is that the so-called "superposition principle" will remain valid [5,6]. According to this, the charging current density is equal in magnitude to the discharge current density, J_d (cf. Fig. 1) so that

$$J_0(t) - J_\infty = J_d(t) \tag{2}$$

Non-linear polarization

Non-linear polarization is usually caused by the blocking of charge-carriers at the electrode/sample interface. This effect is conceptually similar to the electrochemical polarization effects encountered at electrode/solution interfaces. Theoretical treatments of current-blocking effects at electrode/electrolyte interfaces are available in the literature [7–10]. Solutions and simplifying assumptions underlying the formulation of the non-linear differential equations relating the polarization (and its time derivatives) to the electric field (and its time derivatives) have been given by previous authors [7–10]. In this case, the true conductivity of the material is given by its initial conductivity, σ_0 which is given by the expression [5]

$$\sigma_{true} = \sigma_0 = \frac{J_0}{E_a} = \frac{J_\infty}{E_a - E_p} \tag{3}$$

where E_p is the electric field caused by the space-charge polarization. A value for E_p is difficult to obtain by direct experiment so that the final conductivity, σ_∞ has no simple interpretation unlike in the previous case of linear polarization.

Ohm's law and the superposition principle will not be obeyed in the presence of non-linear polarization so that a plot of ln J_∞ versus ln V (where V is the applied voltage) will be a straight line of slope > 1.

EXPERIMENTAL

Samples of Green River oil shale were collected from three different locations in the tri-state area: the U.S. Department of Energy mine at Anvil Points, Colorado; the Geo-kinetic field test site located south of Vernal, Utah; and the Laramie Energy Technology Center field test site (Site 10) located near Rock Springs, Wyoming. Further details on the origin of these shales and procedures for the preparation of test samples are given elsewhere [11,12]. The Kentucky oil shale samples were obtained from the Sweetland Creek member of the New Albany deposits [13]. Oil yields of the various shale samples were obtained from pulsed NMR assay and specific gravity measurements as described elsewhere [12,13]. The shale samples were employed in the form of right circular thin cylindrical discs (nominal dimensions: 2.23 cm diameter and 0.3–1 cm in thickness) for the current–voltage measurements.

The circuitry employed for the current–voltage measurements is illustrated in Fig. 2. A Hewlett-Packard d.c. regulated power supply (Model 6522A) was used for applying the desired voltage to the test sample. The currents were monitored on a Keithley (Model 616) electrometer in conjunction with a Tektronix oscilloscope.

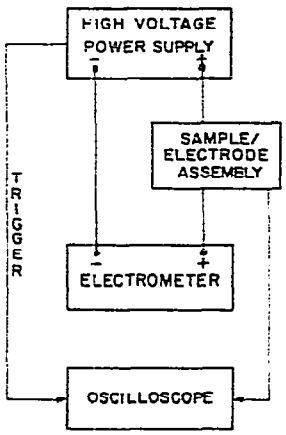

Fig. 2. Block diagram of experimental set-up for current–voltage measurements on oil shales.

Only the final currents (cf. Fig. 1) were recorded since it was the relationship of J_∞ to the applied voltage that was of primary interest here. The current transients extended for periods from a few tenths of a second to several minutes depending on the temperature. In a typical measurement, the temperature was rapidly brought to the desired point and then stabilized to within $\pm 1°C$. The d.c. voltage was applied to the test sample while simultaneously triggering the electrometer and the oscilloscope. (Determination of the initial currents was hampered in some cases by the time response of the instrumentation, particularly at low temperatures where the polarization was relatively rapid.) The final current was noted after the transients had died down. This procedure was repeated for each temperature.

The sample holder for these measurements was a conventional two-terminal type and was of similar design to the one used previously for the Dynamic Dielectric Analysis measurements [14,15]. Conducting silver paint was employed on the top and bottom surfaces of the test sample to minimize contact resistance at the sample/electrode interface.

All measurements were carried out in a flowing N_2 atmosphere to preclude spurious effects arising from oxidation of the shale organic matter. For experiments on pyrolyzed shales, the samples were initially heated to $\sim 500°C$ at the rate of $\sim 10°C\ h^{-1}$ and then maintained at this temperature for approximately 2 h. The samples were then cooled back to room temperature before the actual experiment.

RESULTS

Figures 3–6 illustrate typical current–voltage characteristics for Colorado, Utah, Wyoming, and Kentucky shales, respectively. It is apparent from these data that an

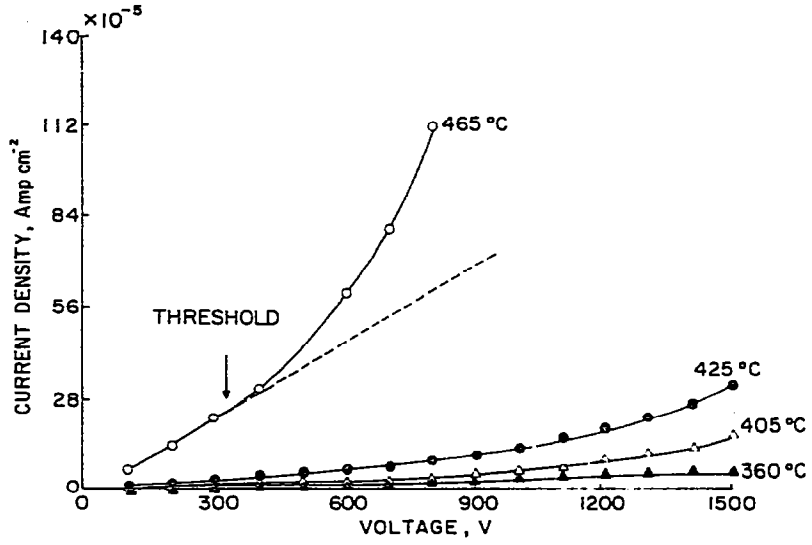

Fig. 3. Variation of current–density with voltage for a Colorado shale sample (oil yield = 200 l tonne^{-1}). Temperature is shown as the parameter.

increase in temperature enhances the non-linearity in the current–voltage relationship; i.e. the voltage at which the current density starts to depart from linear behavior (cf. Fig. 3) is shifted to lower values with increasing temperature. This trend is illustrated in Table 1 where the "threshold voltage" is shown as a function of temperature for the various shale samples.

The influence of shale oil yield (expressed as the number of liters of oil that can be extracted from one metric ton of the shale) and prior thermal treatment (pyrolysis of organic matter) was examined for the Colorado shales. An increase in the shale

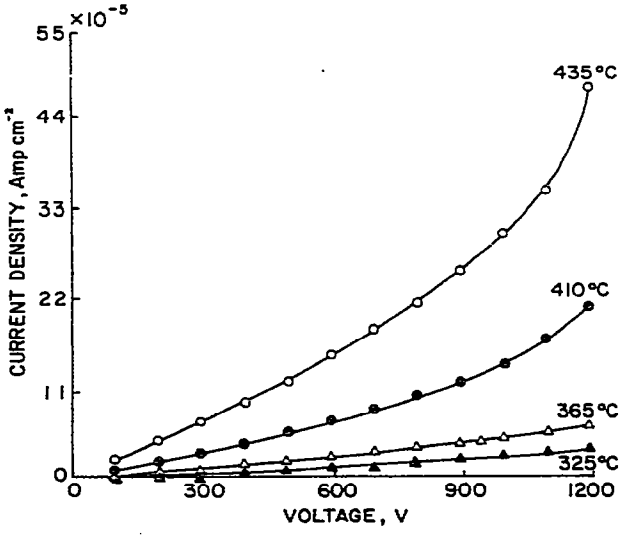

Fig. 4. Variation of current–density with voltage for a Utah shale sample (oil yield = 96 l tonne^{-1}). Temperature is shown as the parameter.

TABLE I

Variation of the threshold voltage (see text for definition) with temperature for eastern and western U.S. shales

Oil shale Oil yield	Temperature (°C)	Threshold voltage [a] (V)
Colorado		
68 l tonne^{-1}	280	>1500
	325	>1200
	425	>1200
	475	600
	530	300
Colorado		
68 l tonne^{-1} (pyrolyzed)	275	>1200
	375	900
	470	430
	510	220
Colorado		
200 l tonne^{-1}	280	>1500
	365	>1500
	405	900
	425	810
	465	300
Colorado		
340 l tonne^{-1}	280	>1050
	330	750
	380	520
	425	375
Utah		
96 l tonne^{-1}	225	>1200
	325	>1200
	365	900
	410	600
	435	515
Wyoming		
96 l tonne^{-1}	320	>1125
	360	>1125
	430	1050
	470	600
	510	400
Kentucky		
88 l tonne^{-1}	410	>900
	455	>900
	485	600
	510	300

[a] Nominal error in measured value = ±50 V.

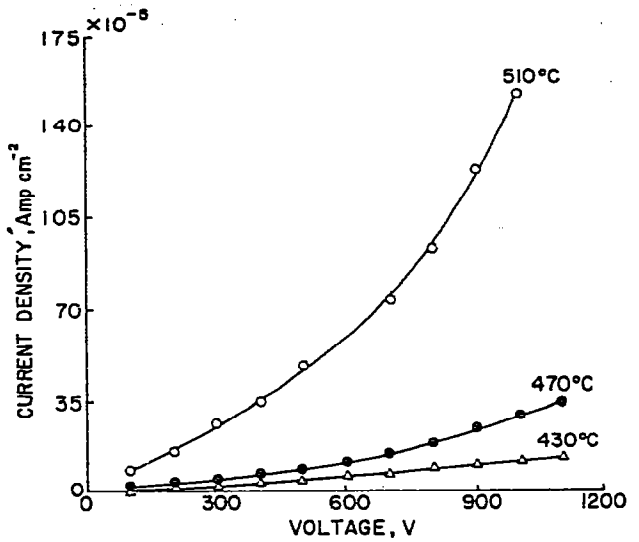

Fig. 5. Typical current density–voltage characteristics for Wyoming shales. The sample had an oil yield of 96 l tonne^{-1}. Temperature is shown as the parameter.

organic content (or oil yield) tends to enhance the non-linearity in the current–voltage behavior. This is manifested by the shift in the threshold voltage to lower values with increasing oil yield at a given temperature (compare the data at 280 and 425°C for the 68, 200, and 340 l tonne^{-1} samples in Table 1).

Figures 7–9 illustrate typical plots of ln J_∞ vs. ln V for Colorado, Wyoming, and Utah shales, respectively. The characteristic slopes obtained from least-squares fitting of the data in such plots are assembled in Table 2 for selected samples. Two regions of different slopes (the first with a slope ~ 1 and the second of slope ~ 2) are

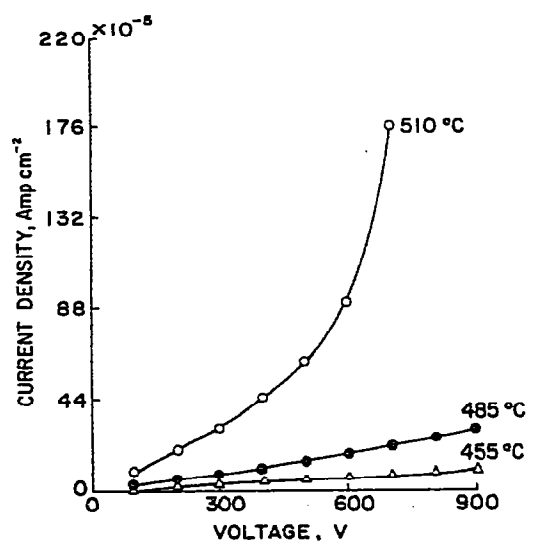

Fig. 6. Variation of current density with voltage for a Kentucky shale sample (oil yield = 88 l tonne^{-1}). Temperature is shown as the parameter.

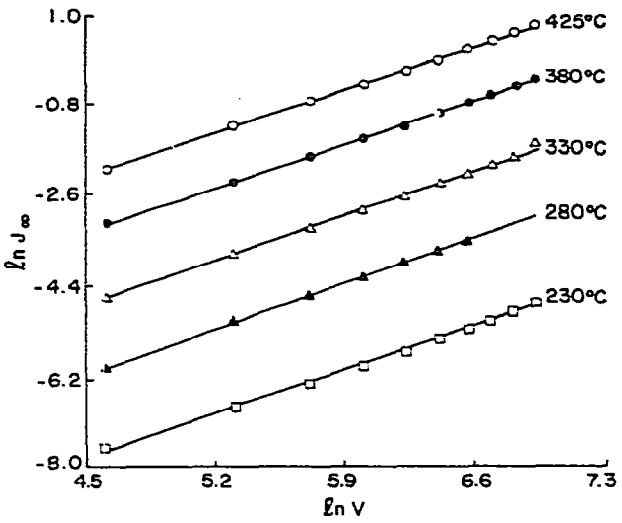

Fig. 7. ln–ln plots of the current–voltage characteristics for the 340 l tonne^{-1} Colorado oil shale sample

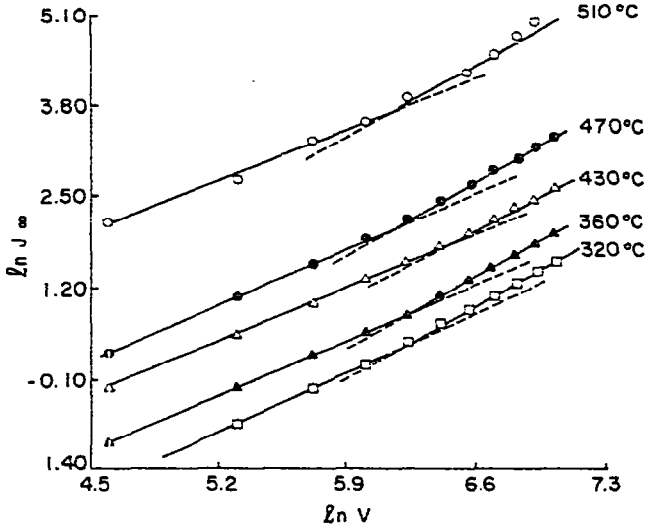

Fig. 8. ln–ln plots of the current–voltage characteristics for the 96 l tonne^{-1} Wyoming oil shale sample.

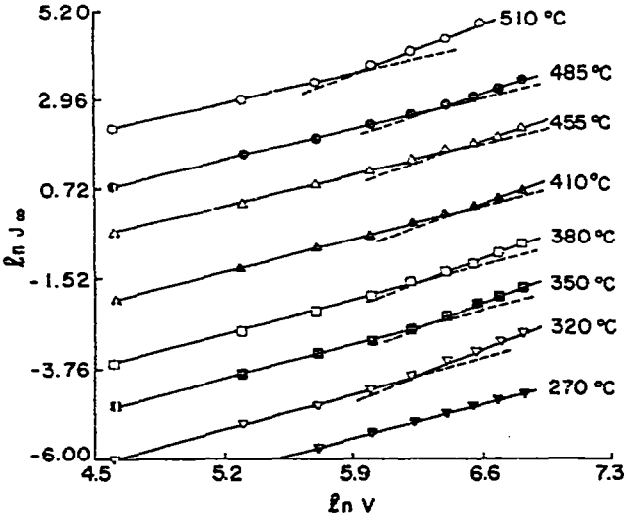

Fig. 9. ln–ln plots of the current–voltage characteristics for the 88 l tonne^{-1} Kentucky oil shale sample.

TABLE 2

Characteristic slopes of current–voltage curves (cf. Figs. 7–9) for eastern and western U.S. shales

Sample Oil yield	Temperature (°C)	Characteristic slope [a]	
		n_1	n_2
Colorado			
68 l tonne^{-1} (raw)	325	1.30	
	425	1.18	
	475	1.22	
	530	1.24	
68 l tonne^{-1} (spent)	275	1.23	1.94
	450	1.18	1.78
	470	1.05	1.90
	510	1.09	2.29
200 l tonne^{-1}	125	1.24	
	280	1.27	
	405	1.21	2.11
	425	1.08	2.09
	465	1.17	2.06
340 l tonne^{-1}	230	1.25	
	280	1.32	
	330	1.31	
	380	1.29	
	425	1.26	
Kentucky	270	1.42	
	320	1.36	1.85
	350	1.34	1.89
	380	1.34	1.88
	455	1.12	1.60
	510	1.06	1.73
Wyoming	320	1.22	1.48
	360	1.15	1.49
	430	1.34	1.40
	470	1.16	1.50
	510	1.06	1.52

[a] Nominal error is measured value $= \pm 0.02$.

n_1 and n_2 denote slopes, cf. equation $\ln J_{\infty} = n_1 \ln V + n_2 \ln V$.

apparent in the data in Figs. 8 and 9 and in Table 1. The second region is absent in some cases (e.g. 68 and 340 l tonne^{-1} Colorado shales, Table 1). Prior thermal treatment of the shale sample results in the emergence of this second region as evidenced by the data on the 68 l tonne^{-1} shale sample.

Reversal of the polarity in the applied voltage did not significantly affect the nature of the trends in the data.

DISCUSSION

A convenient method of distinguishing between linear and non-linear mechanisms involves examination of ln J_∞ vs. ln V plots (cf. Figs. 7–9). As mentioned in a preceding section, linear polarization will result in plots with a slope of +1 whereas non-linear polarization yield linear ln J_∞ vs. ln J plots of slope > 1. The present data on oil shales reveal a complex behavior involving both linear and non-linear polarization effects. Only a highly simplified model can be offered to rationalize the present results. Development of a more comprehensive model must await further elucidation of the nature of the charge carriers and the detailed chemistry of the reactions at the sample/electrode interface.

The data in Table 1 unequivocally show that an increase in temperature shifts the threshold voltage (delineating J–V regimes of linear and super-linear behavior) to lower values for all the shale samples examined in the present study. We attribute this trend to the influence of temperature on the electrical conductivity of the material. In this regard, we need to distinguish between the cases of raw shales vis-à-vis the pyrolyzed samples. In the case of raw shales, an increase in temperature enhances the conductivity in two ways. This may be understood on the basis of the equation

$$\sigma_{\text{true}} = Ne\mu \tag{4}$$

where N is the number of charge carriers, e is the electronic charge and μ is the carrier in ability. Pyrolysis of the organic matter in the shale is expected to create polar fragments [4] so that an increase in temperature will tend to enhance the magnitude of N in eqn. (4). An additional contribution to this increase may arise from the increased mobility and dissociation of water molecules bonded to the clays in the shale matrix. The second factor in the increase in σ_{true} with temperature concerns the mobility term in eqn. 4. The temperature dependence of μ may be expressed in the usual manner [5]

$$\mu \alpha \frac{1}{T} \exp\left(-\frac{\phi_m}{kT}\right) \tag{5}$$

where ϕ_m is the activation energy for charge transport and other terms have their usual significance. The exponential dependence of μ on temperature will probably tend to dominate the overall influence on σ_{true} except perhaps at elevated temperatures (> 400°C) where the pyrolytic reactions attain fast rates [16].

In the case of the pyrolyzed shale samples, only the mobility effect (represented by eqn. (5)) is expected to play a significant role in the increase of σ_{true} with temperature since no chemical reactions occur whereby new charge-carrying species are created (this is strictly true only over the temperature change 25–~600°C. At higher temperatures, dissociation of the carbonate minerals will tend to have profound effects on N and therefore on the measured σ_{true} values).

Returning to the influence of temperature on the current–voltage characteristics (cf. Figs. 3–6, Table 1) an increase in temperature results in a concomitant increase in the rate at which charge carriers are supplied to the electrodes for reasons noted

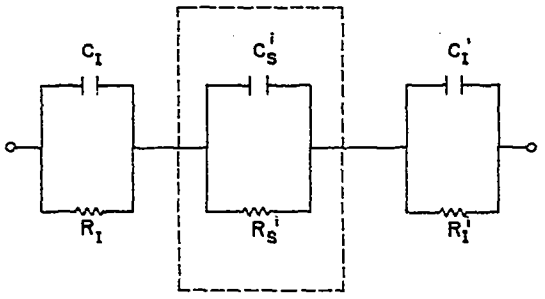

Fig. 10. Equivalent circuit representation of oil shale. C_I, C_I' and R_I, R_I' represent capacitive and resistive elements, respectively, of the space-charge layers at the two electrode/sample interphases. C_S^1 and R_S^1 denote the composite capacitance and resistance terms corresponding to the bulk shale sample. The non-homogeneous and multi-phase nature of the shale result in a network of parallel R_SC_S terms combined in series (not shown in the figure).

above. The finite rate of discharge of these carriers at the two electrodes sets up space-charge layers in the immediate vicinity of the sample/electrode interface. These layers may be represented by capacitive and resistive elements as illustrated in the equivalent circuit in Fig. 10. The occurrence of carrier blocking at the electrodes will result in field distortion and consequently in non-linearity in the $J-V$ characteristics.

An increase in the shale organic content also results in a shift in the threshold voltage to lower values although the effect is somewhat less dramatic than that observed with temperature. We interpret this shift to arise from changes in the electrical conductivity of the material with a change in its organic content. Previous studies in this laboratory had established a correlation between the dielectric loss tangent and organic content for Green River oil shales [12]. Although these results pertain to microwave frequencies (>1 MHz), roughly the same trends may be expected to hold in the d.c. case, if account is taken of the diminishing influence of the displacement current term with decreasing frequency. Because of the increased conductivity, space-charge polarization brought about by carrier blocking at the electrodes will set in at a lower voltage relative to the case of a material with lower conductivity values (vide supra).

The occurrence of a second region of slope ~ 2 in the $\ln J_\infty$ vs. $\ln V$ plots for the pyrolyzed shale sample and the absence of this region in the raw material (Table 2) are indicative of the importance of chemical composition in determining the type of polarization mechanisms in the material. The formation of a carbon residue from pyrolysis of the shale organic matter can account for the difference in behavior between the raw and pyrolyzed shale samples. A thin layer of carbonaceous residue in the immediate vicinity of the electrode will tend to impede carrier discharge and thereby enhance the space-charge polarization effect. Such a layer is roughly equivalent to the introduction of additional resistive and capacitive elements in series with the RC term corresponding to the interface layer (cf. Fig. 10).

We then have the following simplified model for the oil shale matrix. Under the influence of an electric field, the charge carriers migrate to the two electrodes where

they are discharged via electrodic charge transfer reactions. The greater the conductivity of the bulk material, the faster are the carriers supplied to the respective electrodes and the lower the value of the threshold voltage at which space-charge (non-linear) polarization sets in. Temperature and shale organic content are two key factors in determining the extent to which blocking of charge carriers at the electrodes affects the current–voltage characteristic. Compositional homogeneity of the bulk material also seems to play a critical role. The presence of resistive carbon particles formed as a residue in the pyrolytic reactions and consequently a greater degree of mineral/carbon particle contacts result in an additional source of space-charge polarization at these boundaries. Although under normal circumstances, space-charge polarization within the bulk material results in a linear current–voltage relationship (cf. ref. 17), it is quite possible that the field distortion in heterogeneous materials such as shales, will be large enough in the interior of the sample to induce non-linearity. This bulk polarization effect is also expected to diminish in importance with increasing organic content of the shale such that bulk conductivity and interfacial electrode/sample charge transfer become major factors (vide supra). It is pertinent to note that these effects are accompanied by an anomalous increase in the capacitance of the shale samples as reported previously [2].

ACKNOWLEDGEMENTS

The author acknowledges the able assistance of M. Das in the experiments reported here.

REFERENCES

1 D.A. Northrup, Sandia Labs. Rep., UCRL 52227, 1975.
2 K. Rajeshwar, R. Nottenburg, J. DuBow and R. Rosenvold, Thermochim. Acta, 27 (1978) 357.
3 R.N. Nottenburg, K. Rajeshwar, R.J. Rosenvold and J. DuBow, Fuel, 58 (1979) 144.
4 K. Rajeshwar, M. Das and J. DuBow, Nature (London), 287 (1980) 131.
5 P.H. Sutter and A.S. Nowick, J. Appl. Phys., 34 (1963) 734.
6 S.W.S. McKeever and D.M. Hughes, J. Phys. Chem. Solids, 39 (1978) 211.
7 G. Jaffé, Ann. Phys., 16 (1933) 217, 249. G. Jaffé, Phys. Rev., 85 (1952) 354. H. Chang and G. Jaffé, J. Chem. Phys., 20 (1952) 1071. G. Jaffé and C.Z. LeMay, J. Chem. Phys., 21 (1953) 920.
8 J.R. Macdonald, Phys. Rev., 92 (1953) 4. J.R. Macdonald and M.K. Brachman, J. Chem. Phys., 22 (1953) 1314. J.R. Macdonald, J. Chem. Phys., 22 (1953) 1317; 23 (1955) 275, 2308; 29 (1958) 1346; 30 (1958) 806.
9 R.J. Friauf, J. Chem. Phys., 22 (1954) 1329.
10 P.W.M. Jacobs and J.N. Maycock, J. Chem. Phys., 39 (1963) 757.
11 K. Rajeshwar, R.J. Rosenvold and J. DuBow, Ind. Eng. Chem., Prod. Res. Dev., 19 (1980) 629.
12 K. Rajeshwar, J. DuBow and R. Thapar, Can. J. Earth Sci., 17 (1980) 1315.
13 K. Rajeshwar and J. DuBow, Fuel, 59 (1980) 737.
14 K. Rajeshwar, R.N. Nottenburg and J. DuBow, Thermochim. Acta, 26 (1978) 1.
15 R. Nottenburg, K. Rajeshwar, M. Freeman and J. DuBow, J. Solid State Chem., 28 (1979) 195.
16 K. Rajeshwar, R.N. Nottenburg and J. DuBow, J. Mater. Sci., 14 (1979) 2025.
17 M.M. Perlman, J. Appl. Phys., 42 (1971) 2645.